In-Board Magnetics Processes

Yi E. Zhang
yizhang@crown.eecs.berkeley.edu
Tel: (510)-643-5895

Seth R. Sanders
sanders@eecs.berkeley.edu
(510)-642-4425

Fax: (510)-642-2739
Department of Electrical Engineering and Computer Sciences
University of California, Berkeley
Berkeley, CA94720 U.S.A.

I. Introduction

This paper introduces a design and manufacturing process for integrating magnetic components, transformers and inductors, within a multilayer printed circuit board (PCB). As such, the magnetic core constitutes one or more of the layers of the PCB, as illustrated in Fig. 1. This structure has a number of potentially advantageous features. The thickness of the resulting magnetic component can be rather small, comparable to that of standard laminated multilayer PCB's. If the traces used to form the turns of the magnetic devices are internal layers of the multilayer PCB, the surface real estate occupied by the magnetic device is fully available for other surface mountable components. Thus, this technology offers great advantage in packaging density. In addition, the planar type form factor provides for a large surface area to volume ratio, allowing for effective heat transfer from the magnetic device.

This paper provides a design methodology for in-board magnetic devices. Specifically, we evaluate various magnetic core materials, focusing on magnetic metal alloys which can be patterned by chemical etching or punching and have mechanical properties that are compatible with PCB processes. Our design process encompasses winding designs that minimize combined core and winding losses. Parasitic components such as leakage inductances are readily evaluated and repeatable. Winding designs can be made to nearly eliminate external magnetic fields. Permeable cores of in-board magnetic components are made of laminations of magnetic metal films. Core loss and permeability can be controlled by selection of material, introducing anisotropy, gapping, and combinations of these.

II. Geometry and Structure of In-Board Magnetic Devices

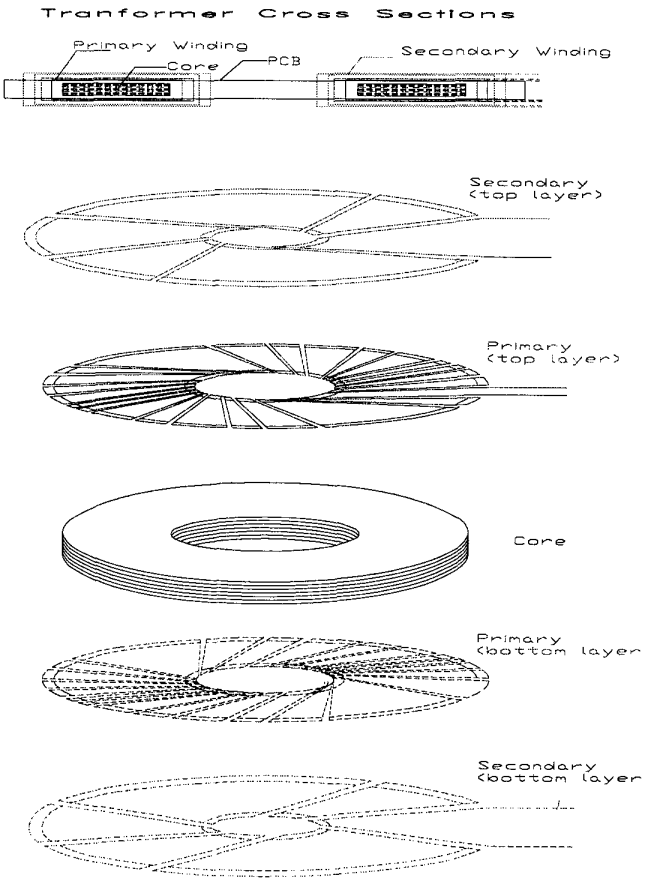

Fig.1 In-board magnetic structure

Fig. 1 shows an in-board magnetic structure, such as would be used in a transformer. Standard multi-layer PCB technology is used with a multilayer magnetic metal core, laminated within the board. Primary and secondary windings are laid out on different layers of the PCB. Cross-sections of each of the copper conductor layers are also shown. Vias, not show in Fig.1, are used to make the winding connections between layers. The

0-7803-5421-4/99/$10.00 © 1999 IEEE

thickness of the copper layers is chosen according to skin depth and manufacturing considerations. For power inductors, no more than two layers of copper are needed. Nevertheless, additional layers can be used to reduce winding resistance in an inductor, and careful layout can be used to null external leakage fields.

III. Magnetic Materials --- Inducing Anisotropy with Bias Field

A core material for power transformers requires all the good properties of a soft magnetic material, e.g. high saturation inductance, high permeability and low core losses. Ideally, the permeability of a core material for a power inductor should be adjustable. Appropriately adjusted permeability allows a gapless design, which avoids losses associated with the gap field and avoids the potential difficulty in manufacturing gaps.

Conventionally, core losses are divided into hysteresis loss and eddy-current loss, with the latter including classical eddy current and anomalous losses. References [1-4] give detailed discussions of hysteresis loss in anisotropic thin films. It is well known that if an ac field is applied in the hard axis direction, the hysteresis loss can be eliminated or at least significantly reduced. We attempt to take advantage of this feature by inducing an anisotropy with an external dc bias field, as detailed below.

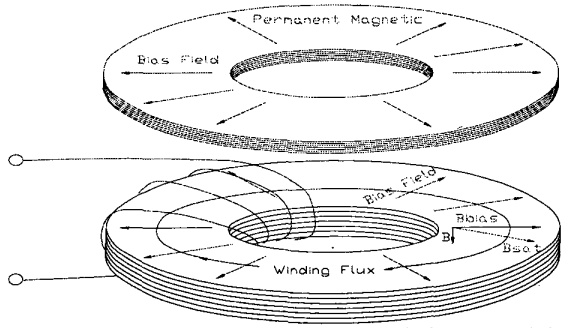

Fig.2. Inducing anisotropy by radially applied dc bias field, with permanent magnetic mounted above core

Fig. 2 shows a ring shape core. If an external dc bias field is applied in the radial direction, an anisotropy (easy axis) can be induced in the radial direction. Assuming the dc bias field is large enough to drive the core into saturation, the amplitude of the flux density will be the saturation flux density B_{sat}. This flux density will be aligned with the applied dc bias field. With toroidal windings, as shown in Fig. 2, the working ac field is applied in the azimuthal direction. Locally, at each point in the core, the flux density vector aligns with the vector sum of the applied magnetic fields, radial dc bias and azimuthal field due to the winding. Thus, we have the azimuthal component of flux density

$$\vec{B}_\phi = \frac{\vec{H}_\phi}{\left|\vec{H}_\phi + \vec{H}_{bias}\right|} B_{sat} = \mu_{eff} \vec{H}_\phi$$

where H_{bias} and H_ϕ are intensities of the radial dc bias field and the azimuthal field due to the windings, respectively. It is easy to see that if the bias field is increased, the effective permeability μ_{eff} is decreased.

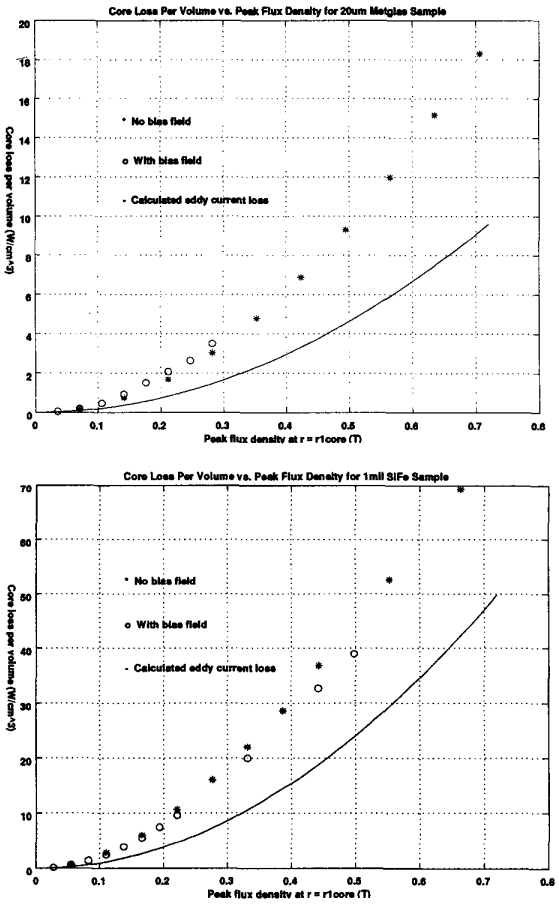

Fig. 3 Core loss density for (a) Metglas 2705 and (b) Silicon Steel, both at 300KHz. Data points marked with asteriks taken with zero bias field. Data points marked with circles taken with bias field. Curve shown corresponds to theoretical eddy current loss.

The advantages of incorporating such a dc bias field are:

1) The required inductance value can be achieved by adjusting the bias field (and hence also effective permeability). Gapping may be avoided.

2) As the permeability becomes smaller, the skin depth increases. This allows better flux penetration at high frequencies. Thus, fewer layers, but of thicker material may be used in a given design.

3) The bias field can introduce a strong anisotropy, and a corresponding hard axis in the azimuthal direction. Hysteresis loss can be reduced significantly with this anisotropy.

Fig.3 (a) and (b) shows core loss measurements for 20um thick Metglas and 25um thick silicon steel samples. For the silicon steel sample, when a bias field is applied to the sample, the core loss is reduced due to the induced anisotropy. The Metglas sample has very low hysteresis loss, and hence the difference in loss with and without bias field is comparable with measurement errors. Theoretical eddy current losses are also plotted out on the same axes.

Core loss data was taken from direct power input measurements into a high efficiency soft-switched half-bridge stage, which directly drove a winding applied to the core under test. Losses incurred in the half-bridge circuit were calibrated with appropriately adjusted air core inductor loads.

IV. Transformer and inductor design

Here, we characterize power loss minimizing transformer and inductor designs, as has been done in references [3-4]. Specifically, for a given technology, i.e. copper thickness, core layer thickness, numbers of copper and core layers, designs that optimally trade-off copper and core losses are developed. A strategy for transformer optimization is outlined here. Inductor optimizations are similar, except for the need to consider DC bias flux.

For the purposes here, we assume that core losses are dominated by eddy current loss. This assumption is motivated by the situation where an anisotropy is introduced that makes hysteresis losses negligible, as discussed in Section III. Thus eddy current core losses are approximated by:

$$P_{core} = \frac{w^2 d^2 h_s}{24 \rho_s} \int_{r_{1core}}^{r_{2core}} B(r)^2 * 2\pi * r dr \qquad \text{(IV-1)}$$

where w is the frequency in radians/sec, d is the thickness of each lamination, h_s is the total height of the core, ρ_s is the resistivity of the core material, and r_{1core} and r_{2core} are inner and outer radii of the core, respectively. Equation (IV-1) is the classical eddy current loss integrated over volume.

The flux density is inversely proportion to the radius, and it can be derived from:

$$B(r) = \frac{V_2}{4 f N_2 h_s \ln\left(\frac{r_{2core}}{r_{1core}}\right)} * \frac{1}{r} \qquad \text{(IV-2)}$$

where V_2 is the secondary voltage, N_2 is number of secondary turns, f is the frequency, and B_1 is the peak flux density at $r=r_{1core}$.
Combining (IV-1) and (IV-2), we obtain

$$P_{core} = \frac{\pi^3 V_2^2 h_s}{48 \rho_s (\frac{h_s}{d})^2} * \frac{1}{N_2^2 \ln(\frac{r_{2core}}{r_{1core}})} \qquad \text{(IV-3)}$$

Equation (IV-3) is the classical eddy current formula, restated in terms of secondary voltage and number of secondary turns.

The total copper loss is the summation of primary and secondary copper losses. The resistance for radial current flow in an annular shape winding (1 turn, 2 sides) is:

$$R_0 = 2\int_{r_1}^{r_2} \frac{\rho}{2\pi r h_c} dr = \frac{\rho}{\pi h_c} \ln\left(\frac{r_2}{r_1}\right)$$

where r_1 and r_2 are inner and outer radii of the winding respectively. Dividing the above winding into N turns, the width of the winding decreases by N, and the length increases by N. Thus, the resistance is increased by a factor of N^2, yielding

$$R_N = \frac{N^2 \rho}{\pi h_c} \ln\left(\frac{r_2}{r_1}\right)$$

Given that the space between adjacent turns is s, the width of the winding is then reduced by a factor of $1 - \frac{sN}{2\pi * r_{ave}}$. Taking this space into account, the copper loss is given by:

$$P_{copper} = \frac{N_2^2 I_2^2 \rho_{cu}}{h_c \pi} * \left[\ln\left(\frac{r_2}{r_1}\right) \frac{1}{1 - \frac{sN_2}{2\pi * r_{ave}}} + \ln\left(\frac{r_2'}{r_1'}\right) \frac{1}{1 - \frac{sN_1}{2\pi * r_{ave}}} \right]$$

(IV-4)

where I_2 is the secondary load current, ρ_{cu} is the resistivity of copper, N_1 is the number of primary turns, N2 is the number of secondary turns, s is the spacing between adjacent traces on the board, r_1 and r_2 are inner and outer radii of the secondary,

respectively, r_1' and r_2' are inner and outer radii of the primary, respectively, and r_{ave} is the average radius of the core. Note that the trace resistances scale with $\ln(r_2/r_1)$, and that the terms $1 - \frac{sN}{2\pi * r_{ave}}$ in this loss formula accounts for clearance spaces between adjacent traces.

With these loss formulae, an optimization strategy is as follows. Output voltage and current levels are specified. Parameters such as number of core laminations and copper thickness are defined by the technology. For a range of outer radii, combined core and copper loss is then minimized, by optimally adjusting the inner radius dimension and the number of turns. More intuitively, if we ignore the space between windings, the copper loss is approximately proportional to $N_2^2 \ln(\frac{r_{2\,core}}{r_{1\,core}})$ while the core loss is inversely proportional to $N_2^2 \ln(\frac{r_{2\,core}}{r_{1\,core}})$. Then the combined core and copper loss is approximately minimized when the copper and core losses are equal. This process is automated in a Matlab routine where second order effects (winding spaces, etc.) are taken into account.

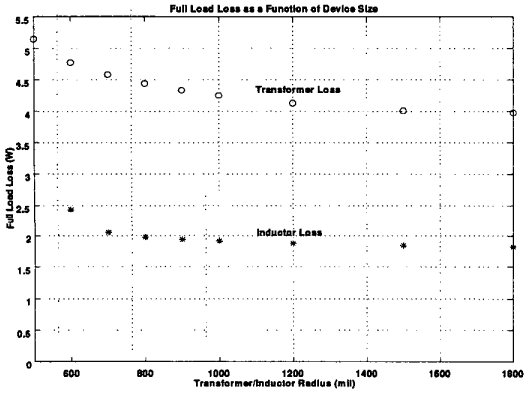

Fig.4 Trade-off between size and efficiency, in 200W transformer and inductor designs

Fig. 4 illustrates a typical output of the design program, for both transformers and inductors. For each outer radius, the total computed loss is displayed. It turns out that the loss approaches a minimal finite value with arbitrarily large radius. A desired design may be selected from the graph of Fig. 4. For example, if the radius of the core is chosen to be 0.7 inches, for a possible technology (80 20μm-thick layers of Metglas 2705 alloy film, 4oz copper for both primary and secondary windings), the efficiency can reach about 98% for a transformer. Fig. 4 shows inductor designs achieving efficiencies in the range of 99% at full load (200W). The inductor designs rely on 1mil SiFe laminations. Larger radii result in slight efficiency improvements, and also take advantage of greater surface area for cooling.

It turns out that for sufficiently large radii, large enough so that clearance spaces are negligible, the efficiency is approximated by:

$$\eta = 1 - \frac{\pi d}{\sqrt{3}} * \sqrt{\frac{K \rho_{cu}}{h_c h_s \rho_s}} \qquad \text{(IV-5)}$$

where K is a technology-dependent constant, ideally equal to 2 for a transformer, h_s is the height of the core, and h_c is the thickness of the conductor. More specifically, the constant K is used to account for the facts that the transformer has two windings and incompletely uses the board space due to clearance between traces. Parameter K can also be used to account for the ratio of measured core loss to the calculated eddy current loss when such data is available. To improve efficiency η, we can:

1) Increase the number of laminations n; which is proportional to h_s.
2) Use thicker copper, i.e. increase h_c.
3) Use magnetic materials that have higher resistivity, i.e. increase ρ_s.

V. Leakage Considerations

As with other planar type designs, evaluation of leakage inductance can be made with one-dimensional approximations, and once the technology is fixed, very good repeatability can be achieved.

As with other toroidal structures, the in-board magnetic structures can be designed to have minimal external fields. Specifically, in a transformer, the windings can be organized to cancel completely the dipole field which would be associated with either the primary or secondary. A similar strategy can be used in an inductor design, provided multiple layers are available for the winding design.

Consider the example transformer design of Section VI, with turns ratio of 4:1. A straightforward way to connect the primary winding is to join all adjacent turns, as shown in Fig. 5a. This would result in minimal primary resistance. However, external leakage fields and leakage inductance are not minimal because the primary and secondary windings are effectively

not anti-parallel. As shown in Fig. 6, this scheme results in a single azimuthal primary turn and a single azimuthal secondary turn. Since the nominal primary and secondary currents are not equal in magnitude, but rather in the ratio of one-to-four, there results a net azimuthal current. This azimuthal current component creates a dipole leakage field which contributes significantly to the external field and the leakage inductance. The leakage inductance of a single azimuthal turn is approximately given by

$$L_{leakage} = \mu_0 R(\ln(\frac{8R}{w} - 1.75) \qquad \text{(V-1)}$$

where R is the radius of the turn and w is its width [5].

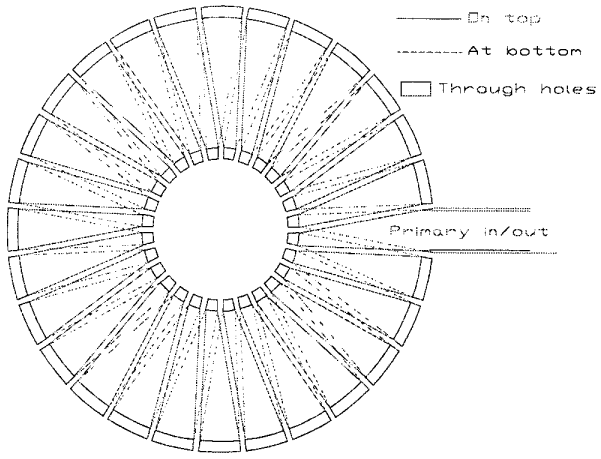

5a. Primary Windings (High Leakage)

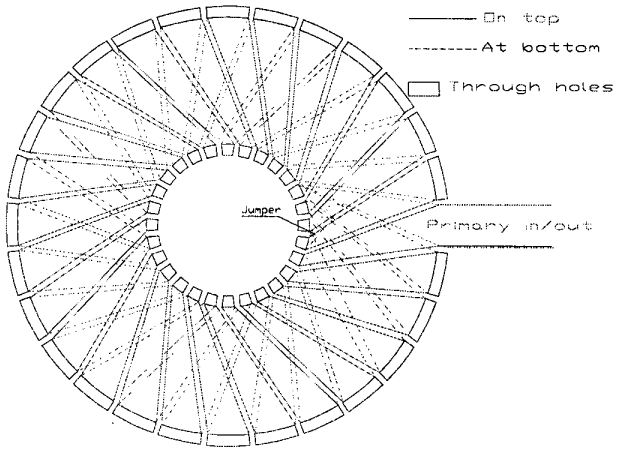

5b. Primary Windings (Low Leakage)

Fig. 5 Two ways to connect primary windings

This component of leakage flux and leakage inductance can be avoided by connecting the primary winding as shown in Fig. 5b. The connection of Fig. 5b organizes the primary winding into four groups of seven turns each. The four groups are interleaved, and connected in series to provide the required 28 turns. Since each of the four groups provides a single azimuthal turn, the primary has four net azimuthal turns. Since the primary current is nominally one-fourth of the secondary current, the result is zero net azimuthal current and no associated dipole field. With this winding scheme the primary and secondary are effectively anti-parallel.

With the scheme of Fig. 5b, leakage inductance can be estimated by calculating the leakage flux between primary and secondary windings.. According to Ampere's law, this field can be approximated by:

$$H_\phi(r) = \frac{NI}{2\pi r}$$

The field is in the azimuthal (ϕ) direction. If h is the space between primary and secondary windings, the leakage flux linkage is approximately:

$$\phi_{leakage} = 2\mu_0 \frac{N^2 Ih}{2\pi} \ln(\frac{r_{2core}}{r_{1core}})$$

where a factor of two accounts for the fact that equal leakage flux occurs on the top and on the bottom of the board structure. Then the leakage inductance referred to the primary is approximately

$$L_{leakage} = 2\mu_0 \frac{N_1^2 h}{2\pi} \ln(\frac{r_{2core}}{r_{1core}})$$

The leakage inductance is directly proportional to the insulation thickness between the primary and secondary windings.

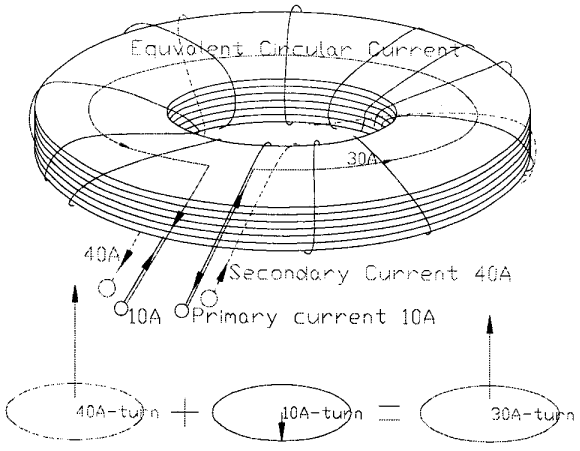

Fig. 6 Dipole leakage flux results from the non-anti-parallel connection of primary and secondary windings of Fig. 5b

In an inductor design, leakage inductance is not an issue, but leakage flux is a source of electromagnetic disturbance. Thus, the same approach may be used to eliminate the dipole field associated with a toroidal inductor if more than one conductor layer is available.

VI. Prototyping and test results

Fig. 7 shows a 200W transformer prototype, corresponding to the point of Fig. 4 for a radius of 0.7 inches. The secondary windings are visible, while the core and primary windings are located within the structure. In this prototype, the laminations of the core have been patterned by laser cutting. Laser cutting is very flexible for prototyping, and can be used to pattern very fine gaps. Fig. 8 shows a laser-patterned silicon-steel lamination, with five gaps, each of 30 microns width.

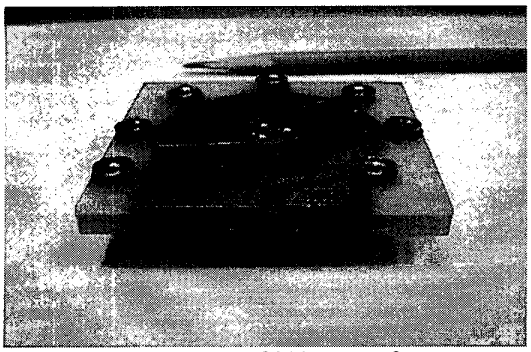

Fig.7. Prototype of 200W transformer

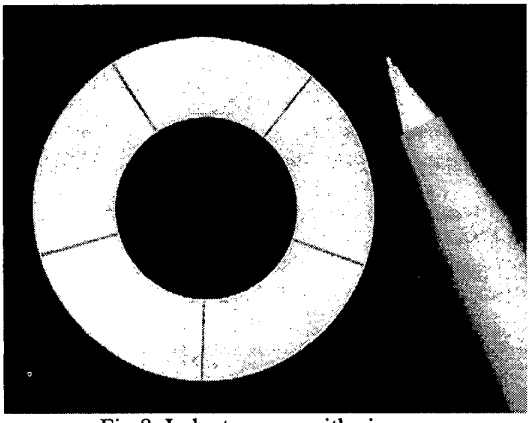

Fig.8. Inductor core with air gaps

Table 1 lists parameters of the prototype transformer shown in Fig. 7. The transformer was designed for application in an active-clamp forward converter, rated for 48V input, 5V output, at 200W. Loss budget for this transformer was approximately 4W at full load. A metglas (2705) core was selected to achieve the core loss necessary to meet this specification.

Symbol	Specifications	Value
f	Frequency	300KHz
V_{in}	Input voltage	±48V
N_1/N_2	Turn ratio	4
I_{out}	Output current	40A
N	Number of core laminations	80
d	Thickness of each core lamination	~20μm
B_{sat}	Saturation flux density	0.77 T
ρ_c	Conductor(Cu) resistivity	1.7μΩ-cm
ρ_s	Core (Metglas) resistivity	136μΩ-cm
h_s	Total height of the core	1.6mm
r_{1core}	Inner radius of the core	327 mil
r_{2core}	Outer radius of the core	700 mil
B_{peak}	Peak flux density at $r=r_{1core}$	0.14T
h_c	Height of the conductor	140μm
δ_c	Skin depth for copper at 300KHz	120μm
h	Insulation space between primary and secondary	125mil
N_1	Primary number of turns	28
N_2	Secondary number of turns	7
r_1	Inner radius of the primary	267 mil
r_2	Outer radius of the primary	760 mil
r_1'	Inner radius of the secondary	207 mil
r_2'	Outer radius of the secondary	820 mil

Table 1 Parameters of prototype transformer

Symbol	Meaning	Calculated	Measured
R_{pri}	DC Primary resistance	52.84mΩ	53.4mΩ
R_{sec}	DC Secondary resistance	4.557mΩ	4.157mΩ
L_s	Primary leakage inductance	750nH	812.8nH
P_{core}	Core loss based on pure eddy current loss model	0.46W @48V input	0.93 @48V input
P_{loss}	Total power loss	2.03W @ 20A output	2.43W @ 20A output

Table 2 Electrical performance of prototype transformer

Test data taken on the prototype transformer is shown in Table 2. Evidently, it is quite practical to meet design values of winding resistance and leakage inductance. Core loss is extrapolated from measured data reported in Section III, and exceeds theoretical eddy current loss by a factor of about two. This was actually taken into account

in the design process where core loss was considered. Thus, the design balances copper and core losses fairly well.

A prototype inductor was also fabricated using the same printed circuit board technology (four conductor layers total) as used for the transformer. The inductor was designed for application as the output choke in the active-clamp forward converter, with maximum load current of 40A. Due to the need to handle large dc flux, a silicon steel core was selected for this application. The design was selected from the data in Fig. 4, with radius of 0.7 inches. Parameters for the prototype inductor are shown in Table 3. The inductor used the four conductor layers to place two five-turn toroidal windings in parallel. The two windings were organized as suggested in Fig. 5b to cancel the azimuthal current and the associate dipole field.

Symbol	Specifications	Value
F	Frequency	300KHz
I_{DC}	DC current	40A
Δi_{pp}	Current ripple	4
N	Number of core laminations	80
D	Thickness of each core lamination	25μm
B_{sat}	Saturation flux density	1.8T
ρ_c	Conductor(Cu) resistivity	1.7μΩ-cm
ρ_s	Core (SiFe) resistivity	47μΩ-cm
h_s	Total height of the core	2mm
δ_s	Skin depth for core at 300KHz	35.9μm
r_{1core}	Inner radius of the core	366 mil
r_{2core}	Outer radius of the core	700 mil
B_{peak}	Peak flux density	1.46T
μ_r	Required relative permeability	308
h_c	Height of the conductor, each of 2layers	140μm
δ_c	Skin depth for copper at 300KHz	120μm
N	Number of turns	5
r_1	Inner radius of winding 1	306 mil
r_2	Outer radius of winding 1	760 mil
r_1'	Inner radius of winding 2	246 mil
r_2'	Outer radius of winding 2	820 mil

Table 3 Parameters of example inductor design

Table 4 reports on measured data for the prototype inductor. As in the case of the transformer, winding resistances match design values fairly well. Core loss is taken from data on silicon-iron laminations, as reported in Section III.

Symbol	Meaning	Calculated	Measured
R_{in}	Inner winding DC resistance	1.65mΩ	1.59mΩ
R_{sec}	Outer winding DC resistance	1.83mΩ	2.01mΩ
P_{core}	Core loss	0.66W @5V output	1.39W @5V output
P_{loss}	Total power loss	1.01W @20A output	1.75 @20A output

Table 4 Electrical performance of example inductor design

VIII. Conclusion and Comments

A novel process for fabricating low profile, high efficiency magnetic components is introduced. Test results match well with simple models. Future versions of the magnetics process will rely on very low profile tape-wound cores, which are likely to result in a still simpler manufacturing process.

References:

1. Jiles, D., *Introduction to magnetism and magnetic materials*. 1st ed. 1991, London ; New York: Chapman and Hall. xxv, 440.
2. Cullity, B.D., *Introduction to magnetic materials*. Addison-Wesley series in metallurgy and materials. 1972, Reading, Mass.,: Addison-Wesley Pub. Co. xvii, 666
3. Daniel, L., C.R. Sullivan, and S.R. Sanders. *Design of microfabricated inductors*. PESC 1996.
4. Sullivan, C.R. and S.R. Sanders, *Design of microfabricated transformers and inductors for high-frequency power conversion*. IEEE Transactions on Power Electronics, 1996. **11**(2): p. 228-38..
5. Ramo, Whinnery, and Van Duzer, *Fields and waves in communication electronics*. 3rd ed. 1994, John Wiley & Sons, Inc.